SAND2018-9760C

Exceptional service in the national interest

Sandia National Laboratories

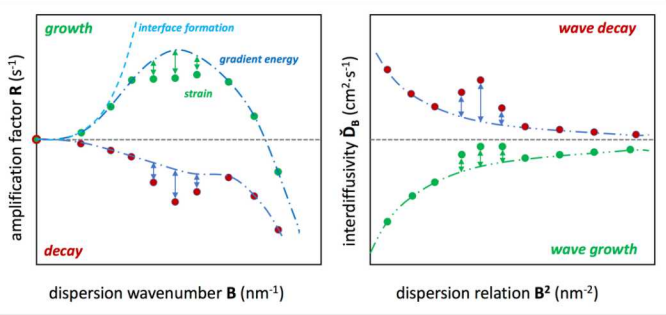

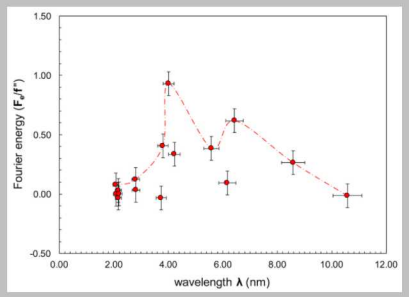

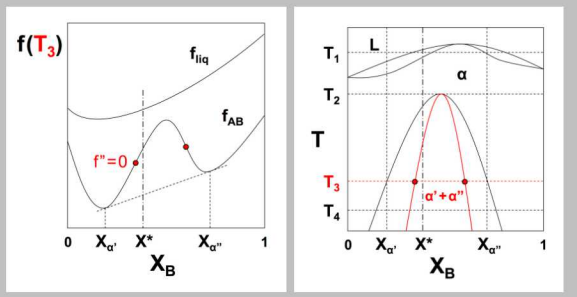

Interdiffusion kinetics in Cu-Ni(Fe) nanolaminate structures

Alan F. Jankowski

U.S. DEPARTMENT OF ENERGY

NNSA National Nuclear Security Administration

Sandia National Laboratories is a multimission laboratory managed and operated by National Technology and Engineering Solutions of Sandia, LLC, a wholly owned subsidiary of Honeywell International, Inc., for the U.S. Department of Energy's National Nuclear Security Administration under contract DE-NA0003525.

Overview

Sandia National Laboratories

- What is a synthetic nanolaminate structure?
  - A metastable structure with an artificial short-range order.
  - Anisotropic physical properties as strength, hardness, magnetism …
  - Nanolaminates are useful to quantify transport properties.
- *The application of interest* – to study the kinetics of the phase transformation for spinodal decomposition at a temperature that is well within the chemical spinodal, i.e. 23°C.
  - The classic Cahn-Hilliard model and Khachaturyan static concentration wave theory are supplemented with a new protocol for analysis of the composition wave fluctuations.
- Results reveal the quantifiable effects of nano structure on the diffusion kinetics.
  - i.e. effects of strain energy and defect structure of the nanolaminates.

Cu-Ni(Fe) nanolaminate

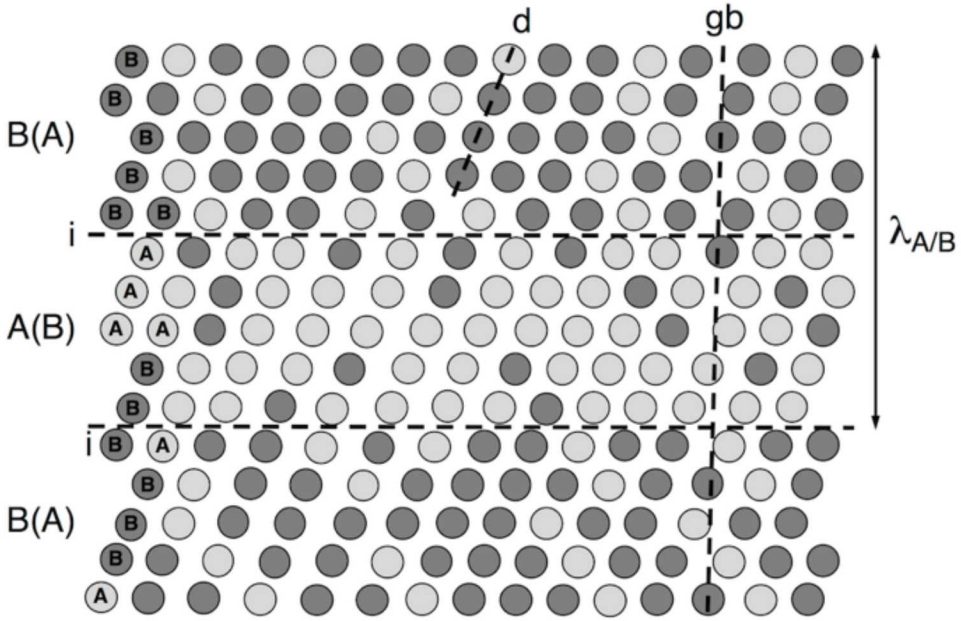

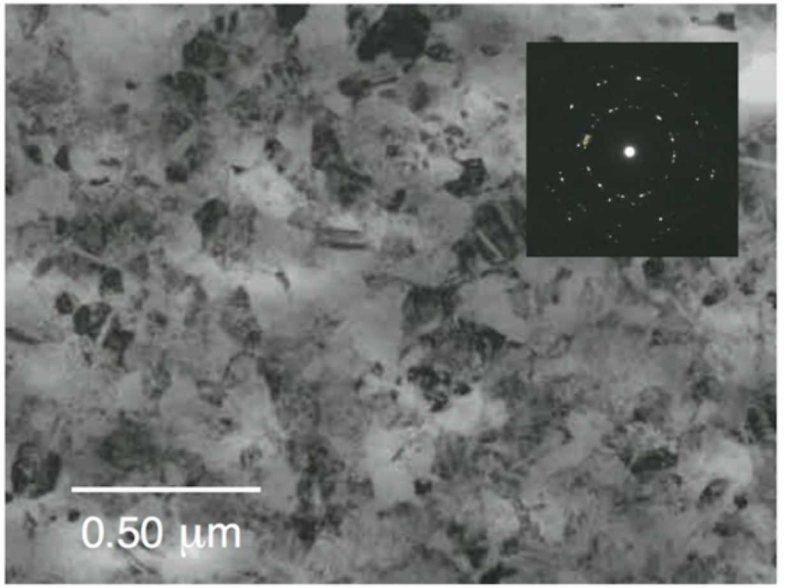

- A laminate of A and B atoms is viewed in cross-section.
  - Features include a threading dislocation (d), a grain boundary (gb) between columnar grains, and the A/B layer pair spacing, i.e. the composition wavelength ($\lambda_{A/B}$).
- TEM BF and SADP images for a nanolaminate with a 4.34 nm composition wavelength reveal its ultra-fine grain nanostructure.

Spinodal decomposition

- Phase separation of an A-B alloy in α-solid solution occurs without a change in crystal structure.
  - The $\alpha \rightarrow \alpha' + \alpha''$ transformation proceeds via uphill diffusion when the 2nd-order derivative of the Helmholtz free energy **f** with respect to composition **c** is less than zero, i.e. $\mathbf{f}'' = \partial^2\mathbf{f}/\partial\mathbf{c}^2 < 0$.
  - The *locus of points* defined by $\mathbf{f}'' = 0$ is the chemical spinodal.
  - It can be shown at a temp **T** beneath the spinodal temperature $\mathbf{T}_s$ that $\mathbf{f}'' = N_v \cdot k_B \cdot (\mathbf{T} - \mathbf{T}_s)/[\mathbf{c} \cdot (1 - \mathbf{c})]$.

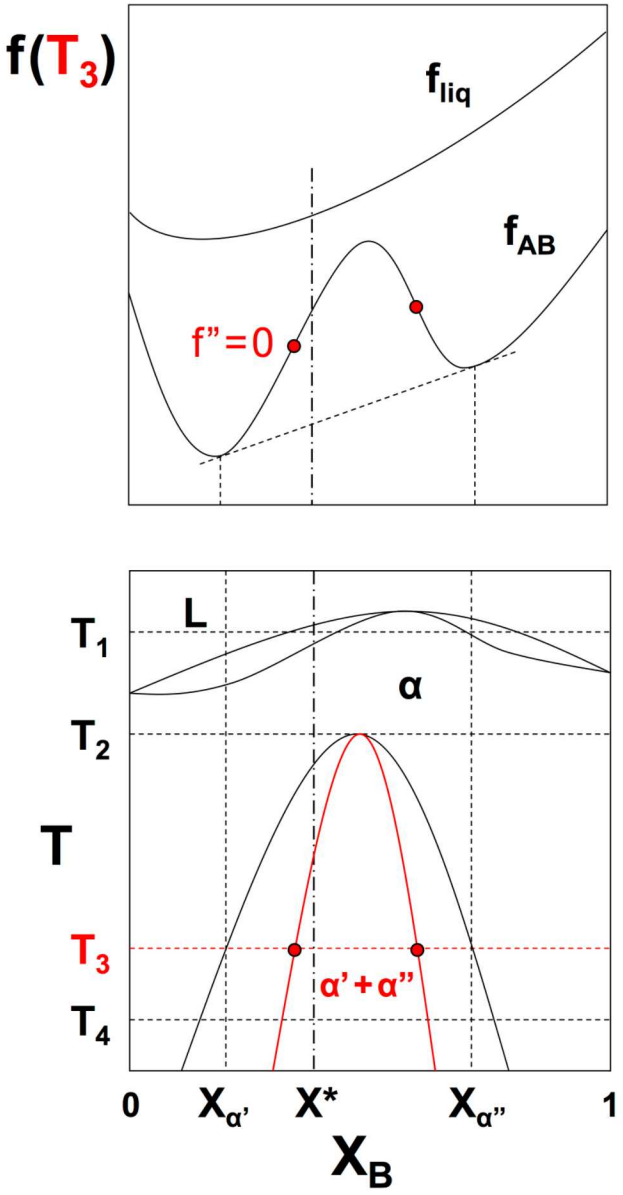

Coherency effects on the spinodal

Sandia National Laboratories

- The Cahn-Hilliard model considers the energetic effects of new interfaces, the composition gradient created, and the presence of interface separation-dependent strain.
  - **R** is used to compute the interdiffusivity $\check{\mathbf{D}}_B$, and model its behavior to determine the diffusion coefficient $\check{\mathbf{D}}(\mathbf{T})$ at a temperature **T**.
  - The decomposition process stops, and decay occurs beyond a critical wavenumber, i.e. $\boldsymbol{\beta} > \boldsymbol{\beta}_c$, where the maximum growth occurs at a wavenumber $\boldsymbol{\beta}_m$ equal to $\boldsymbol{\beta}_c/\sqrt{2}$, and $\boldsymbol{\beta} = 2\pi/\boldsymbol{\lambda}_{A/B}$.
- The presence of strain energy will decrease the composition wave amplitude as quantified by its amplification factor **R**.
  - The energetic effect is to increase the magnitude of interdiffusivity $\check{\mathbf{D}}_B$ outside the spinodal, but decrease its magnitude within the spinodal.
  - A curve fit for **R** using a polynomial expansion of the gradient energy coefficients $\mathbf{K}_\mu$ now allows for the computation of strain energy.

Generalized $\check{D}_B$ equations

Sandia National Laboratories

- The diffusivity $\check{D}$ expressions account for nonlinear effects with time, and are related to the interdiffusivity $\check{D}_B$ through the Fourier transform of the elastic strain energy $F_e(h)$, the second derivative f'' of the Helmholtz free energy per atom volume N_v, and gradient-energy coefficients K_μ.

$$\check{D}_B = \check{D}\cdot\{1 + F_e(h)/f'' + (2/f'')\cdot\Sigma[K_\mu\cdot B^{2\mu}(h)]\} = \check{D}\cdot[1 + \Sigma\, K'_\mu\cdot B^{2\mu}(h)]$$

where h is equal to $d_{(hkl)}/\lambda_{A/B}$ for an interplanar spacing $d_{(hkl)}$,

the dispersion relation $B^2(h) = 2\{1 - \cos(2\pi h)\}/d_{(hkl)}^2$ for cubic metals,

$\check{D} = (M/N_v)\cdot f''$ for the mobility M,

the per atom volume N_v equals $4/a^3$, and $K'_\mu = 2K_\mu/f''$

- The strain energy $F_e(h)$ for the distorted lattice is a function of $B(h)$.

$$F_e(h) = 2\eta(h)^2\cdot Y(h)$$

where the compositionally dependent strain $\eta = (1/a)\cdot(\partial a/\partial c)$, and

Y is the <hkl> orientation-dependent biaxial modulus.

Bounding the wave amplification

Sandia National Laboratories

- The boundary condition of zero amplification at an infinite wavelength is now used to first model the amplification **R** behavior.
  - This step ensures a rigorous computation of $\check{\mathbf{D}}_{\mathbf{B}}$ values, and the subsequent modeling of interdiffusivity behavior to determine $\check{\mathbf{D}}(\mathbf{T})$.
- A higher-order polynomial is fit to the experimental $\mathbf{R}_{exp}$ data to simulate its behavior as $\mathbf{R}_{sim} = \Sigma\, \mathbf{k'}_{\mu} \cdot \mathbf{B}^{\mu}(h)$.
- The $\mathbf{k'}_{\mu}$ terms are then used to compute values for a simulated interdiffusivity $\check{\mathbf{D}}_{B\,sim}$ behavior as $\check{\mathbf{D}}_{B\,sim} = -\mathbf{R}_{sim}/\mathbf{B}^2(h)$.
- The $\Delta\mathbf{R} = (\mathbf{R}_{sim} - \mathbf{R}_{exp})$ and $\Delta\check{\mathbf{D}}_B = (\check{\mathbf{D}}_{B\,exp} - \check{\mathbf{D}}_{B\,sim})$ differences are the consequence of strain energy, and positive quantities at all temperatures.
- From the Cahn-Hilliard formulation, it's now found that the strain energy $\mathbf{F}_e(h)$ equals $\Delta\check{\mathbf{D}}_B \cdot [\mathbf{f}''(h)/\check{\mathbf{D}}]$.
- *With this approach*, the strain energy can be rigorously quantified as a function of the composition wavelength $\boldsymbol{\lambda}_{A/B}$.

Schematic of strain energy effects

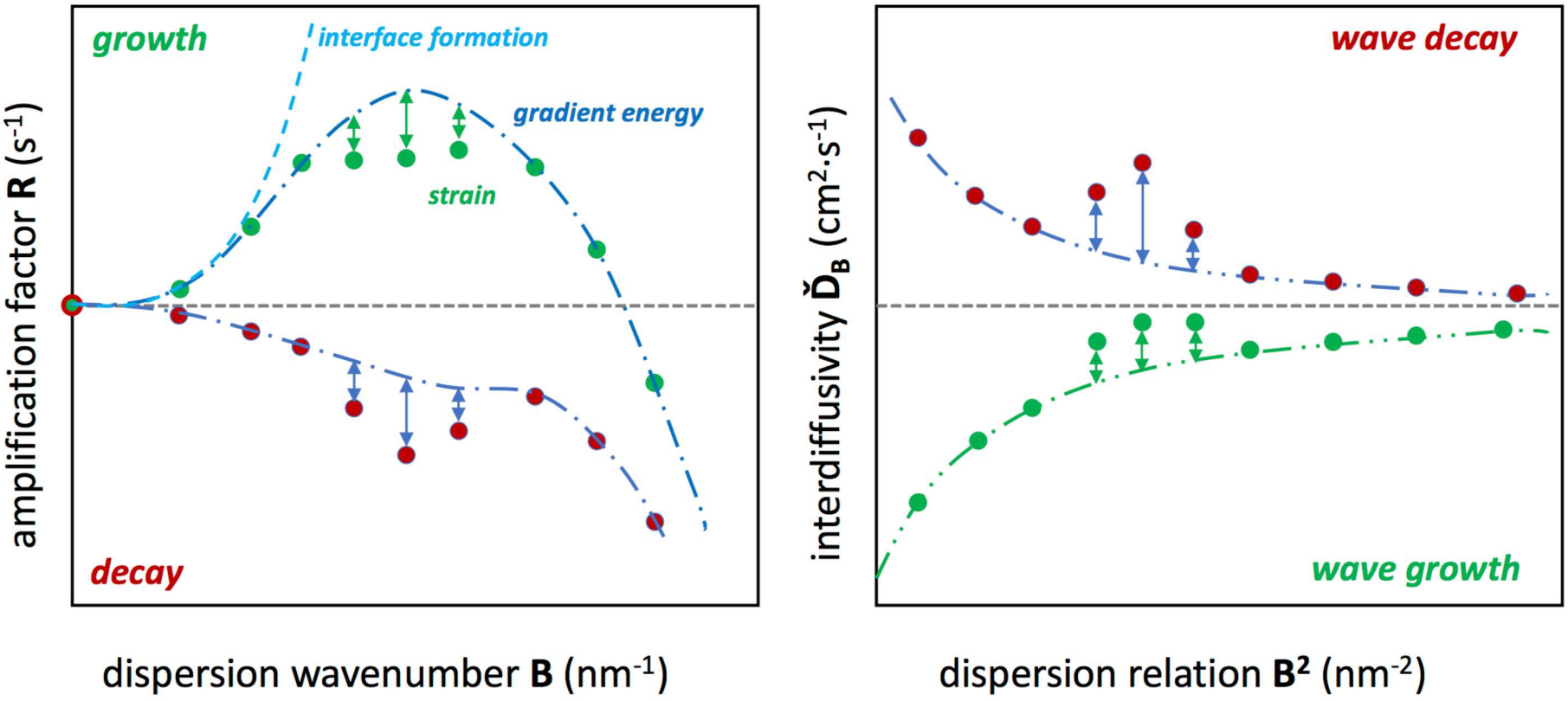

- The polynomial fit envelopes the **R**-data as an upper bound curve.
- The corresponding interdiffusivity $\check{\mathbf{D}}_B$ shows an enhancement of decay to the composition wave; and a slowing of its growth.

Near the Cu-Ni(Fe) spinodal

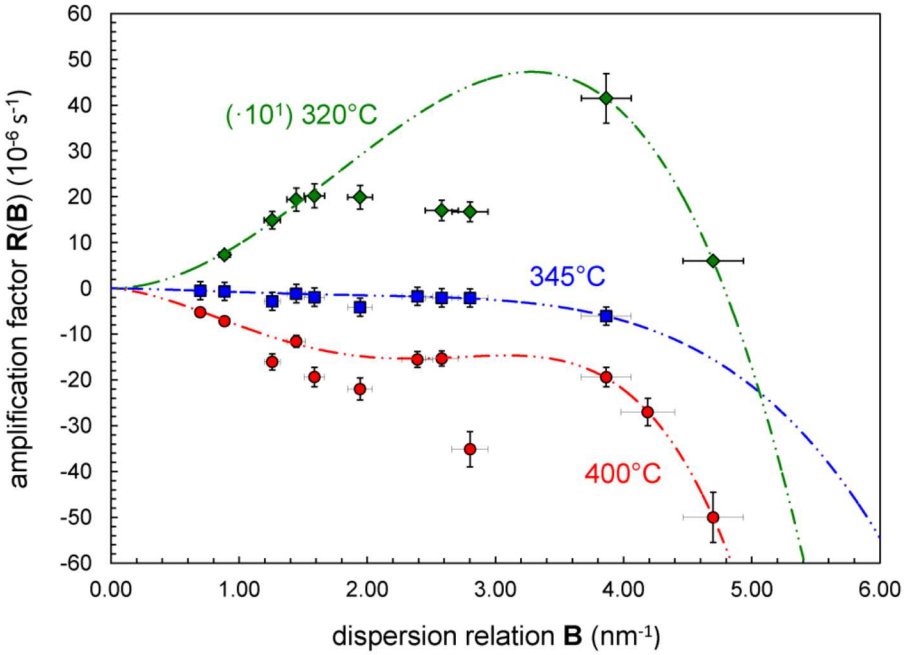

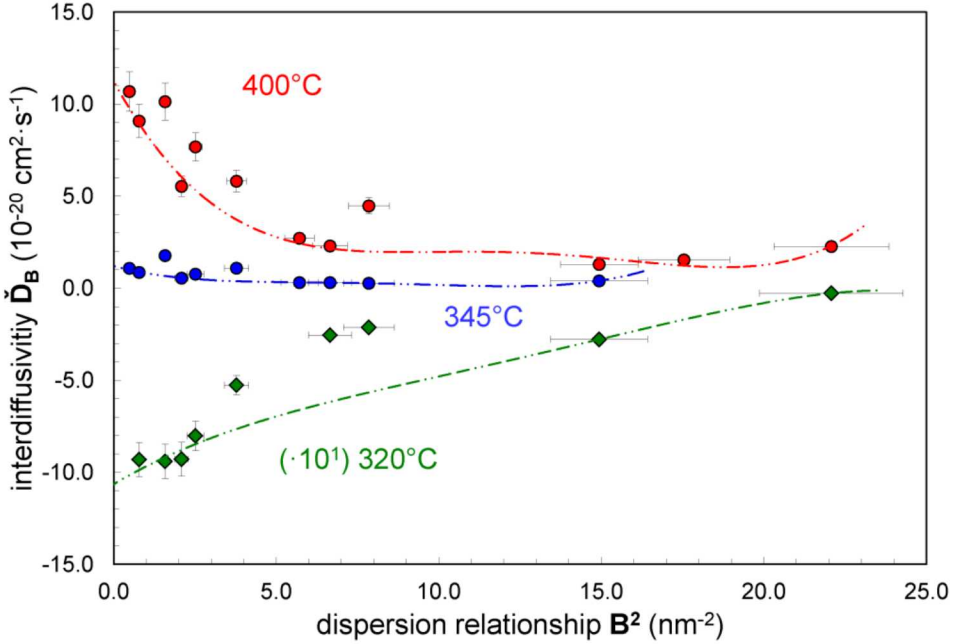

- The interdiffusivity $\check{D}_B$ ($cm^2 \cdot s^{-1}$) variation with the square of the dispersion relation wavenumber B^2 (nm^{-2}) is computed from the amplification factor **R** (s^{-1}) for the Cu/Ni(Fe) nanolaminate samples that were annealed at 320°C (diamond), 345°C (squares), and 400°C (circles).
- The variation from each polynomial fit is due to the effect of strain energy.
- A peak value of $9.4 \cdot 10^7$ $J \cdot m^{-3}$ for the strain energy is computed for the nanolaminate coatings with 2-4 nm composition wavelengths at 400 °C.

θ/2θ X-ray diffraction (XRD) scans

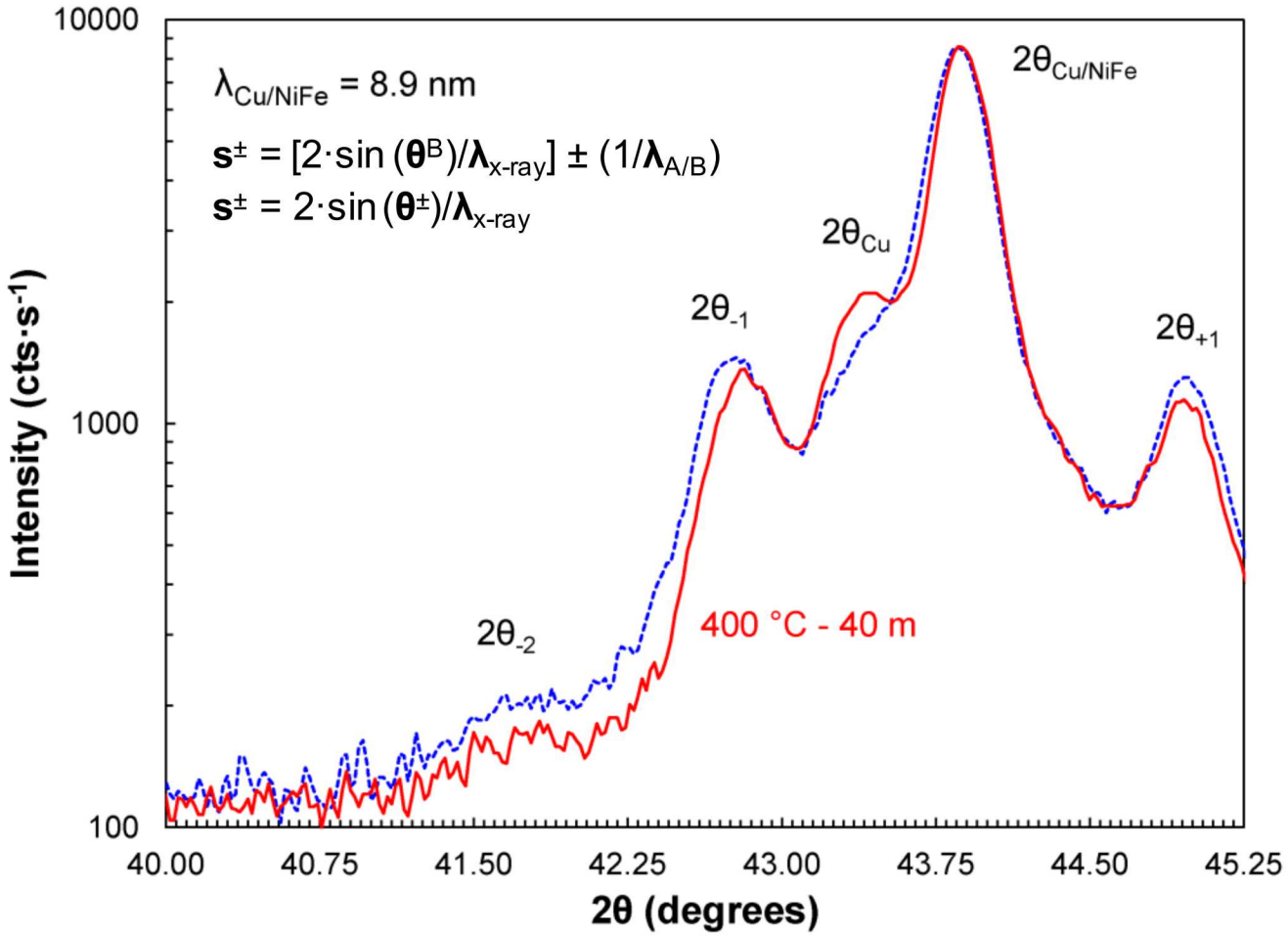

Short-range compositional order produces satellite peaks about the (111) Bragg reflection of the Cu/NiFe nanolaminate. The Bragg peak of the Cu base layer for epitaxial growth is seen.

- The Bragg and satellite peak variation with 2θ position for the Cu/Ni(Fe) nanolaminate coating with a 8.9 nm wavelength **λ** before (dashed line) and after (solid line) a 40 min at 400°C anneal treatment – *decay outside the spinodal*.

θ/2θ XRD scans after 30 yrs

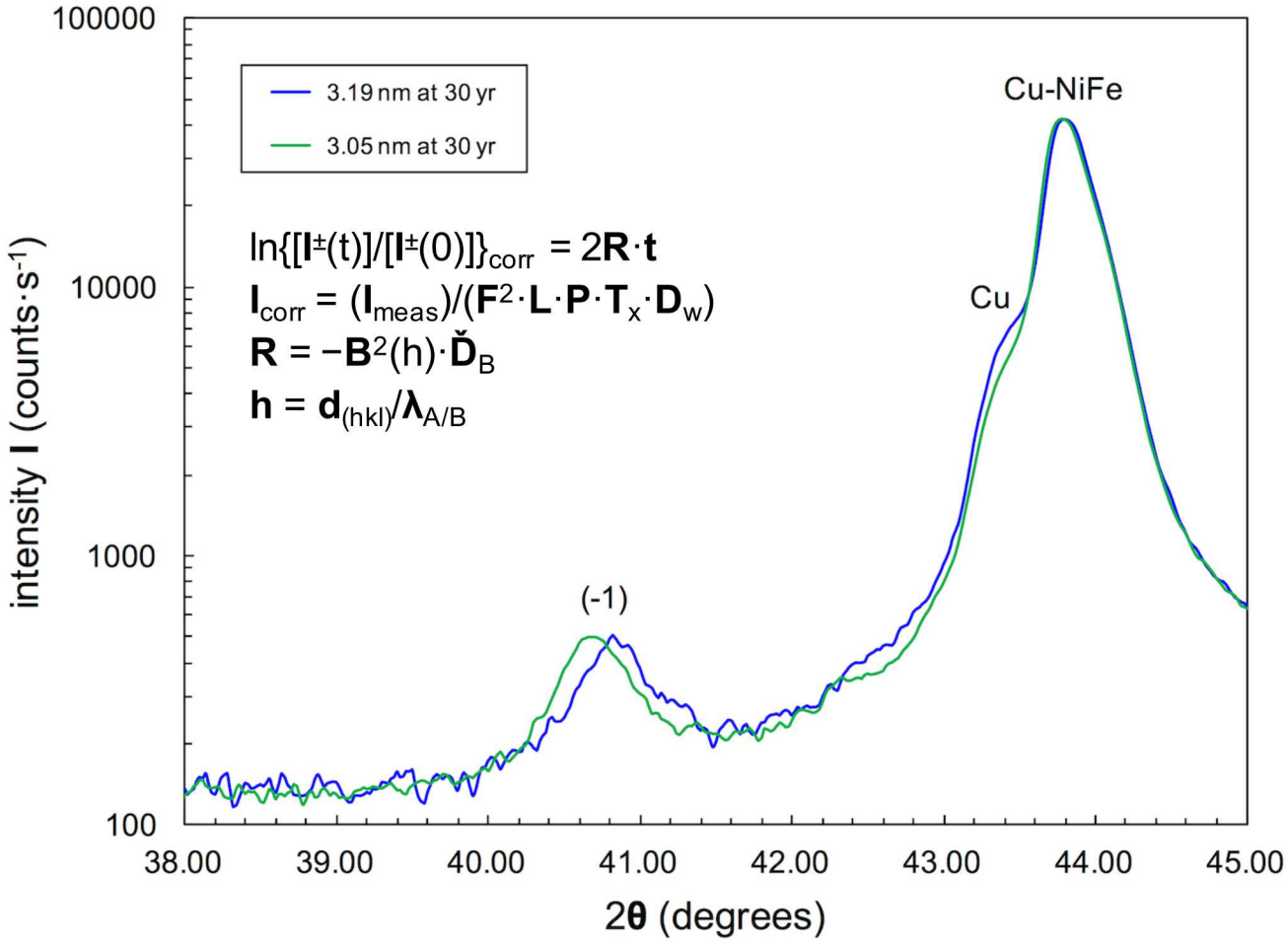

F: composition-averaged atomic scatterings F_i

L·P: Lorentz-Polarization effect as corrected for a graphite monochromator; in this case, at a Bragg angle 2θ of 25°

$\mathbf{T_x}$: product of the mass absorption coefficient μ/ρ with density ρ and specimen film thickness x

$\mathbf{D_w}$: Debye-Waller temperature effect on lattice vibration

- XRD scans of 3.05 and 3.19 nm nanolaminates after 30 yrs at 23°C are shown. The integrated intensity of the satellites are normalized to the Bragg peak intensity.

Table 1. XRD interdiffusivity at 23°C

Sandia National Laboratories

Wavelength λ (nm)		B^2	$(I_{-1}/I_B)_{corrected}$		$R(B)$	$\check{D}(B)$
Initial	Final	(nm^{-2})	Initial	Final	(10^{-10} s^{-1})	(10^{-24} $cm^2 \cdot s^{-1}$)
10.63	10.51	0.35	0.17590	0.18879	0.37	−1.037
8.61	8.54	0.54	0.11493	0.13803	0.94	−1.746
6.46	6.40	0.95	0.06798	0.10785	2.44	−2.563
6.16	6.17	1.04	0.03480	0.07060	3.74	−3.612
5.55	5.61	1.26	0.03427	0.07445	4.10	−3.248
4.34	4.11	2.20	0.01351	0.04003	5.82	−2.648
4.24	3.32	2.43	0.00344	0.00627	3.20	−1.314
4.24	3.37	2.70	0.00959	0.02561	5.19	−1.919
3.68	3.80	2.80	0.00286	0.01136	7.24	−2.588
2.58	3.05	4.91	0.00539	0.01349	4.86	−0.991
2.41	3.19	4.95	0.00413	0.00890	4.05	−0.818
2.22	2.01	8.16	0.00331	0.00955	5.65	−0.692
2.16	2.23	7.97	0.00302	0.00851	5.54	−0.695
2.14	2.19	8.17	0.00156	0.00383	4.71	−0.576
2.10	2.05	8.77	0.00126	0.00221	2.99	−0.341
2.07	2.07	8.90	0.00539	0.00654	1.00	−0.112

- Corrected, integrated-intensities $\mathbf{I}_{corr}$ are used for the initial (t = 0) and final (t = 30 yr) condition to compute **R** – growth is seen within the spinodal.

Wavelength λ (nm) change

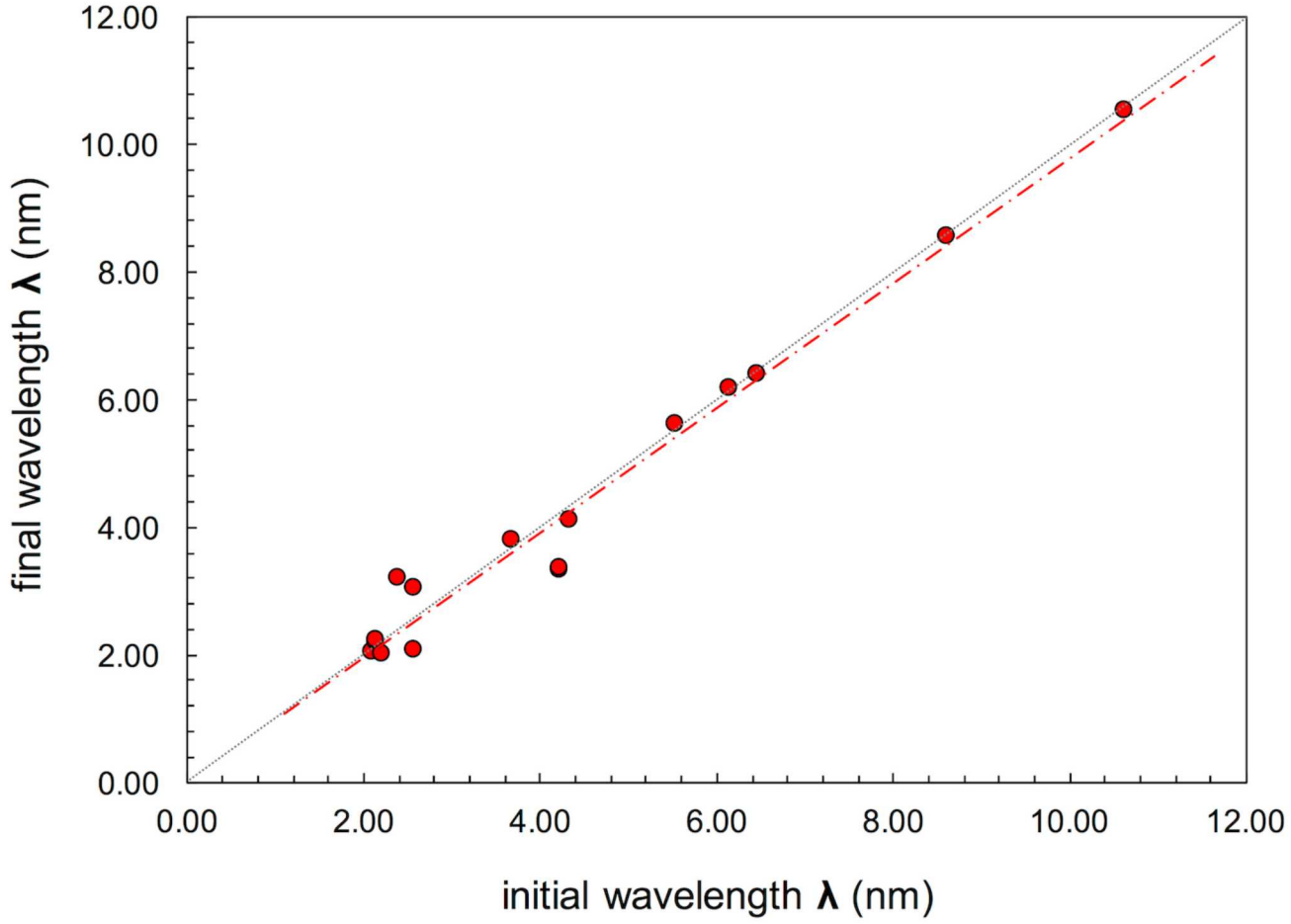

- The wavelength **λ** of the composition modulation after long-term aging is plotted as a function of the initial, as-deposited value for each Cu-Ni(Fe) nanolaminate.

Amplification factor **R** (s^{-1})

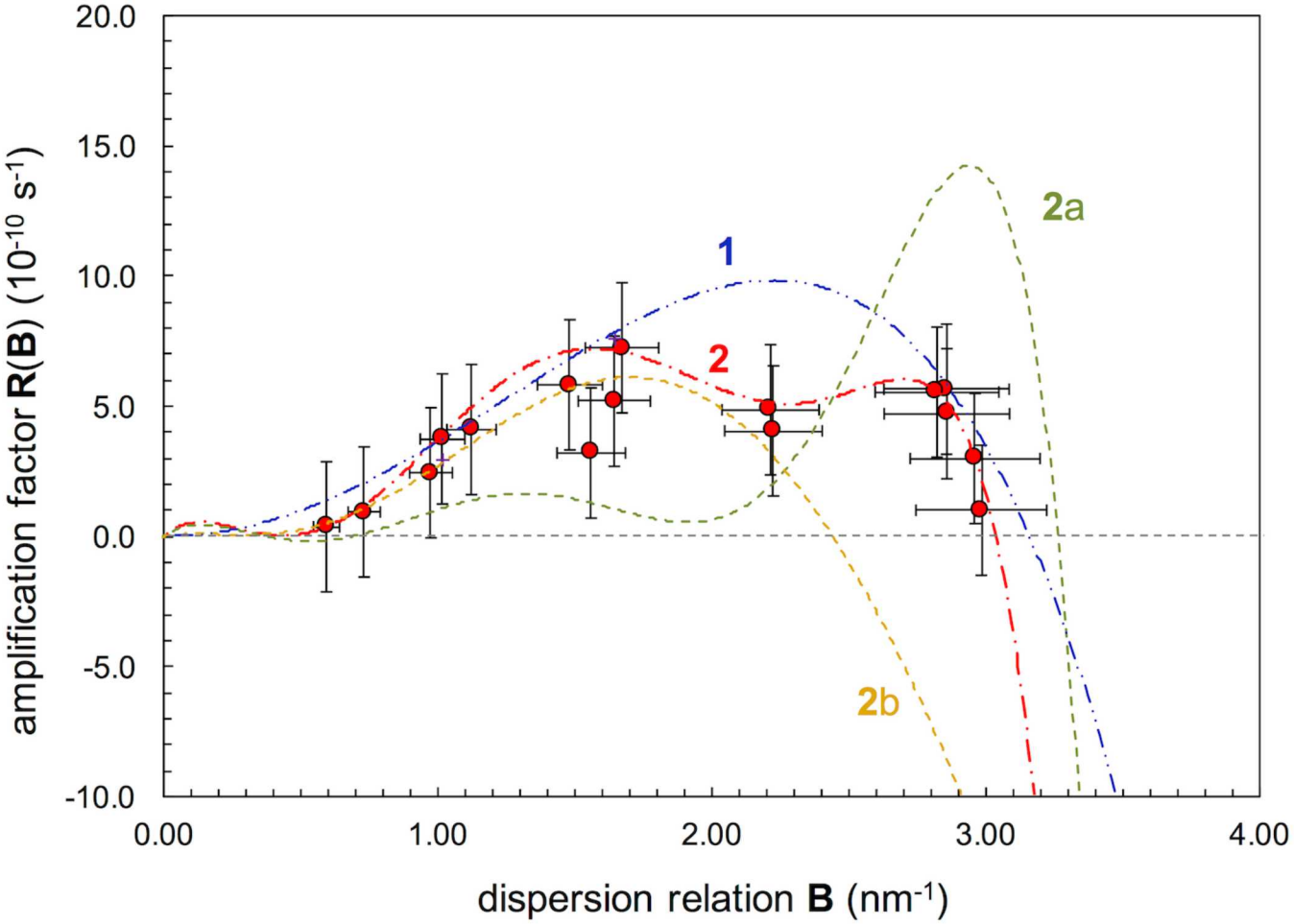

- **R** (s^{-1}) is computed for Cu-Ni(Fe) from changes in the XRD profile. **R** is plotted as a function of the dispersion relation wavenumber **B** (nm^{-1}) in several ways.

Bimodal amplification factor **R**

- The wavenumber β_{max} for the maximum amplification of the composition wave should decrease with time as attributed to nonlinear diffusion as independent of strain energy.
- However, the suppression of the coherent spinodal for long wavenumbers with strain energy contributions will tend to shift the critical wavenumber β_{crit} for allowable growth to greater values since the driving force of the Helmholz free energy increases proportional to the decrease in the process temperature below the chemical spinodal.
- Consequently, the change in β_{crit} would tend to shift the maximum amplification to a larger wavenumber β_{max} although with slower kinetics.

Interdiffusivity $\check{\mathbf{D}}(B)$ ($cm^2 \cdot s^{-1}$)

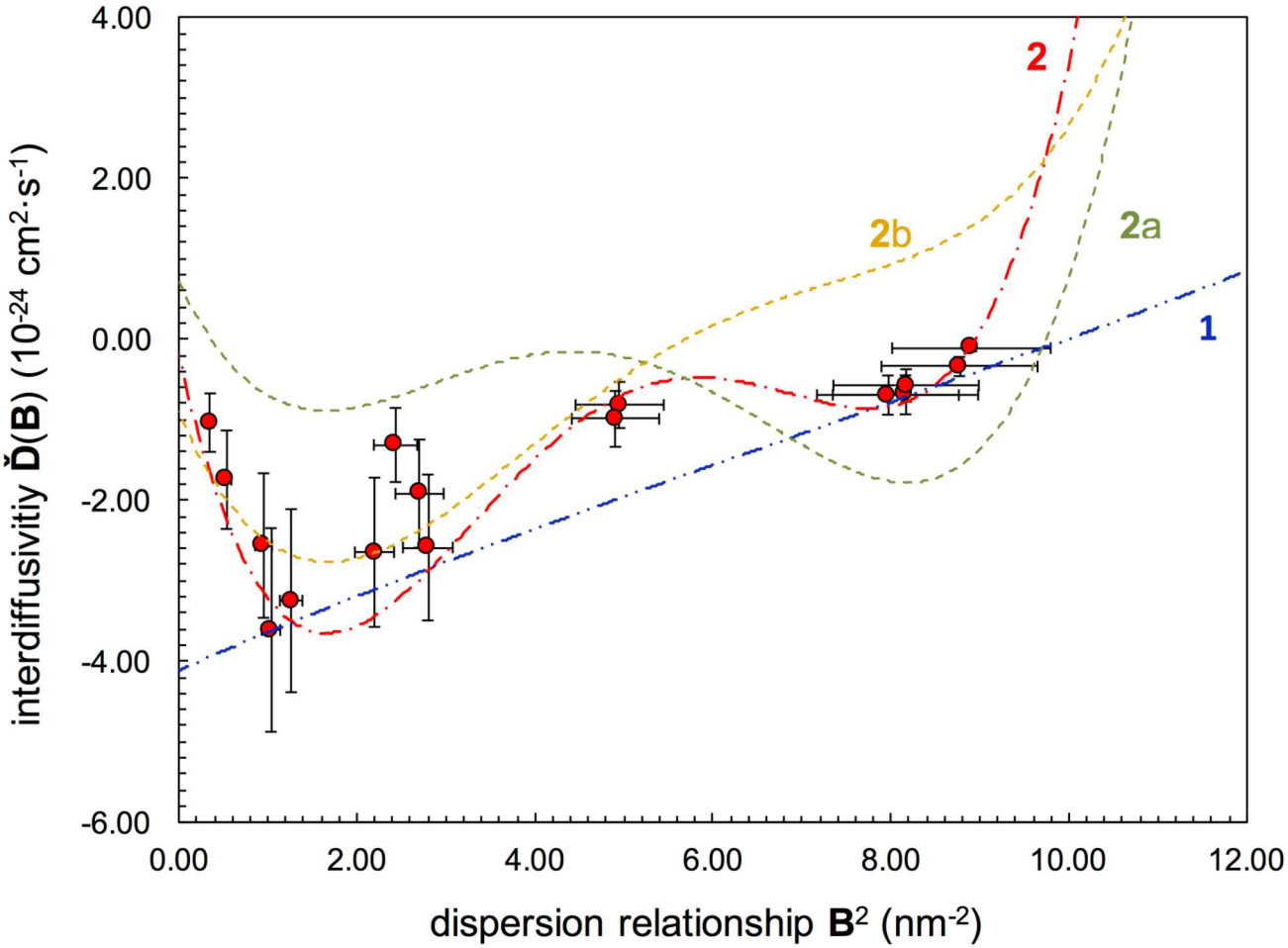

- $\check{\mathbf{D}}$(B) is plotted as a function of the dispersion relationship $\mathbf{B}^2$ (nm^{-2}) for Cu-Ni(Fe) as computed using the tabulated amplification values **R**(B) (s^{-1}).

Table 2. Computed diffusivity and gradient energy coefficients at 23°C

Curve Fit	1	2	2a	2b	3
$\check{D}$ (10^{-10} nm^2·s^{-1})	−4.108	−1.767	0.7208	−0.9222	-1.00×10^{-16}
M (10^{10} nm^2·J^{-1}·s^{-1})	2.383	1.025	−41.82	53.51	5.80×10^{-17}
f'' (10^{-18} J·nm^{-3})	−1.484	−1.484	−1.484	−1.484	−1.484
K_1 (10^{-20} J·nm^{-1})	8.683	−140.2	244.2	−204.1	-1.93×10^{-10}
K_2 (10^{-21} J·nm)	−2.438	711.3	−1166	866.9	1.30×10^{-11}
K_3 (10^{-22} J·nm^3)	1.264	−1106	1945	−1142	-2.35×10^{-12}
K_4 (10^{-23} J·nm^5)	–	554.3	–	506.8	1.36×10^{-11}

- Curve 1: nearly a straight line, as in accordance with a 1st-order gradient energy coefficient **K_1**; a significant deficiency is that the decrease in **$\check{D}$**(B) values which trend below a **B**^{2} value of 1 nm^{-1} can't be reproduced as observed in the experimental data.
- Curves 2a and 2b: constituent curves to the bimodal behavior of curve-2
- Curve 2: correctly envelopes the **$\check{D}$**(B) values; minimizes the Fourier energy component.
- Curve 3: considered for an extrapolated **$\check{D}$** value of $-1 \cdot 10^{-26}$ nm^2·s^{-1} at 23°C for bulk diffusion; required **K_μ** values are computed along with the required order of magnitude for the amplification factor **R**; it's found that the **K_μ** values would have to be 10-to-12 orders of magnitude smaller than values measured, and corresponding **R** values would need to be 16 orders of magnitude smaller than measured.

Fourier energy term ($\mathbf{F_e/f''}$)

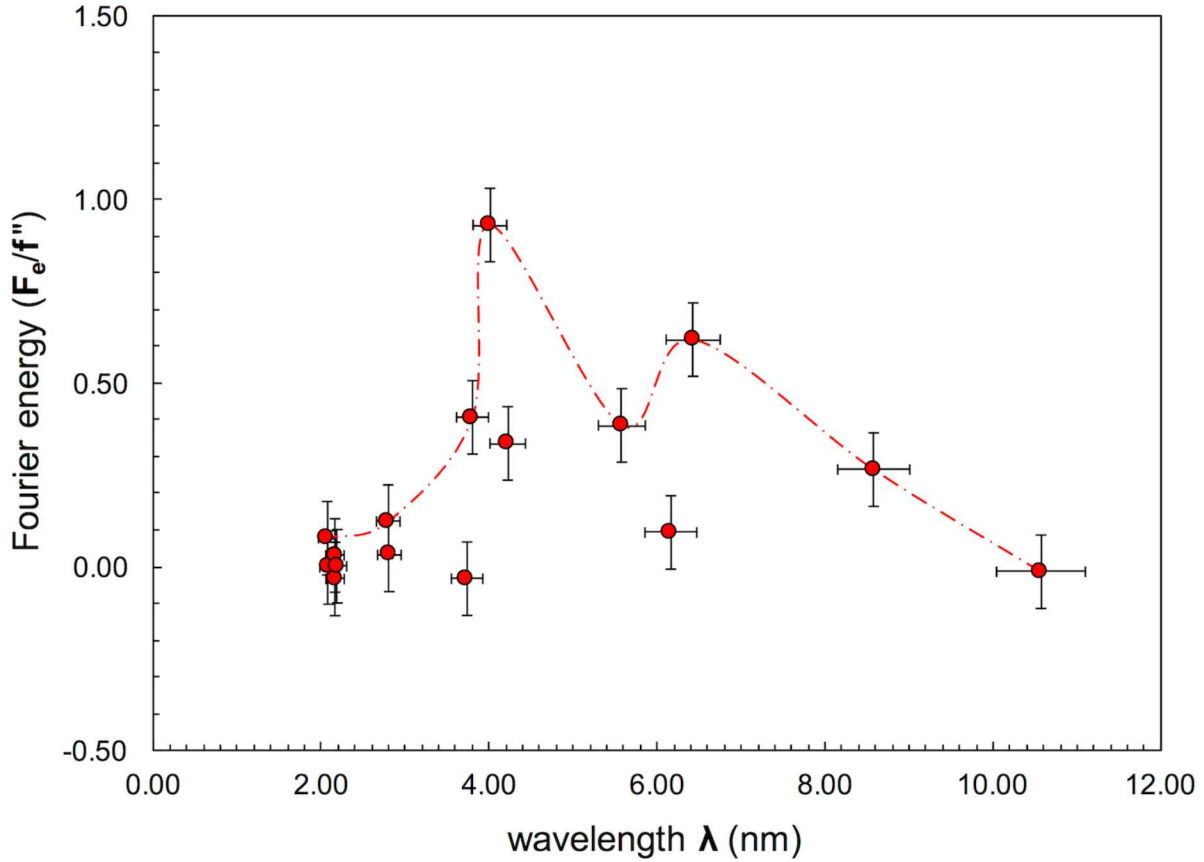

- The Fourier energy computed using the Curve 2 fit for $\check{\mathbf{D}}$(B) provides values for $\mathbf{F_e/f''}$ that are comparable to those reported at 320, 345 and 400°C.
- The local maximum occurs at a composition wavelength consistent with the local maximum in absolute value of the interdiffusivity $\check{\mathbf{D}}$(B) coefficient.

Table 2. Diffusivities at 320-400°C

Material	Cu/Ni(Fe)			
T (°C)	***320***	***345***	***400***	***23***
$\check{D}$ (10^{-6} nm^2·s^{-1})	–1.065	1.208	11.27	$-1.767\cdot10^{-4}$
M (10^{+16} nm^2·J^{-1}·s^{-1})	0.1285	0.2187	0.3139	$1.025\cdot10^{-6}$
f'' (10^{-19} J·nm^{-3})	–0.7134	0.4756	3.091	–14.84
K_1 (10^{-20} J·nm^{-1})	0.3496	–0.9311	–4.494	–140.2
K_2 (10^{-21} J·nm)	–0.2735	1.890	5.752	711.3
K_3 (10^{-22} J·nm^3)	0.1496	–1.702	–3.991	–1106
K_4 (10^{-23} J·nm^5)	–0.0295	0.5397	0.6091	554.3

- Results for 23°C aging are tabulated for comparison with experimental data for **Ď** (cm^2·s^{-1}) from prior experiments at temperatures near the spinodal.
- The bulk diffusivity that would result at room temperature is well below, by 16-orders of magnitude, the anomalously high diffusivity for Cu-Ni(Fe).
- *Next – an assessment of Arrhenius behavior is made with respect to different diffusion mechanisms through the bulk, along dislocations, and at surfaces.*

Arrhenius plot of diffusivity Ď data

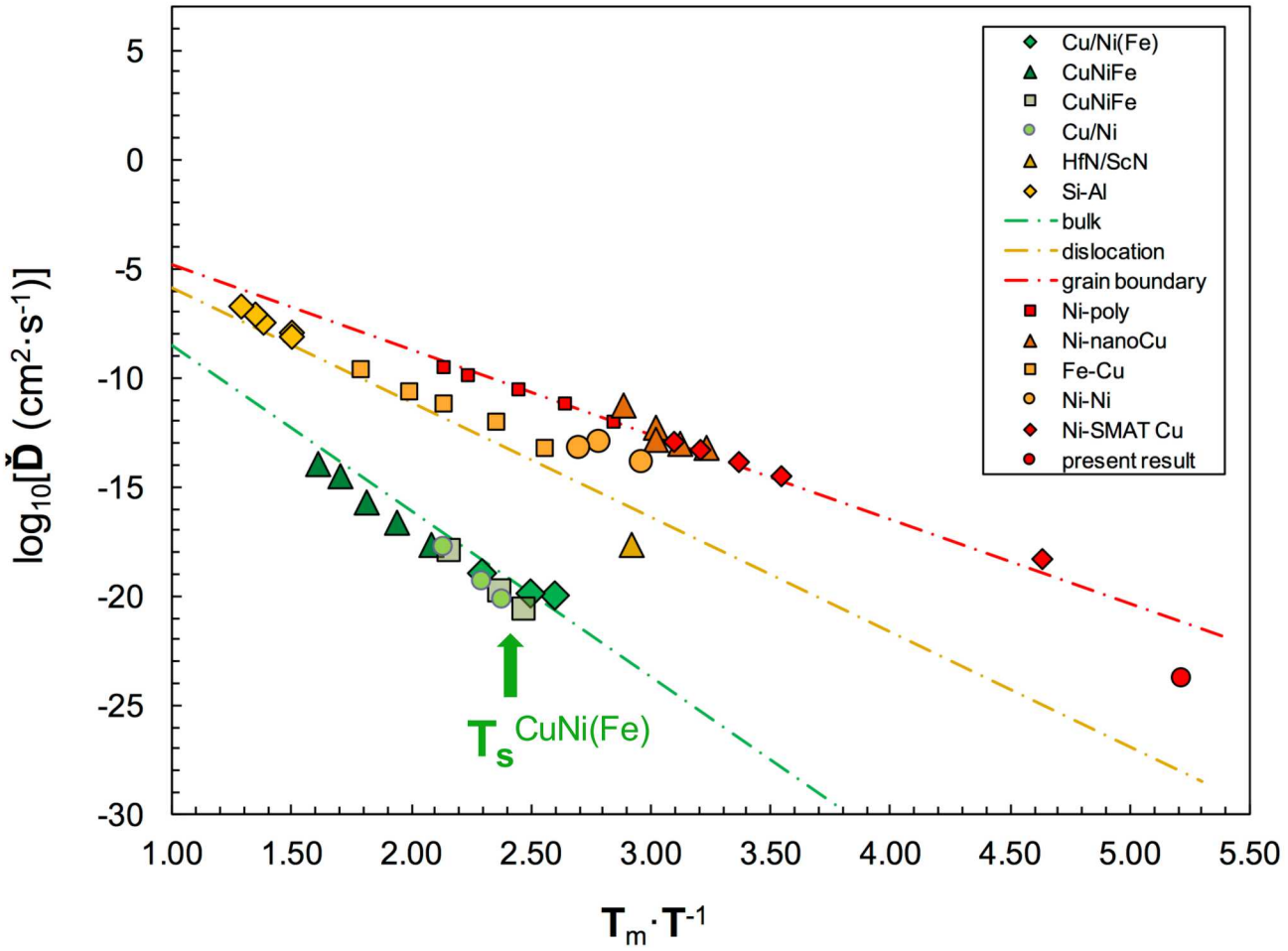

- Linear curves progress with an increasing value of **Ď** ($cm^2 \cdot s^{-1}$) from (lattice or) bulk-, to (dissociated) dislocation-, to (un dissociated dislocation) grain boundary-diffusion as is plotted with respect to the ratio of melt $\mathbf{T_m}$ to test **T**.

Anomalous fast diffusion

Sandia National Laboratories

- Higher diffusion rates become prevalent though the transport of atoms along paths that short circuit the bulk diffusion process.
  - Alternative paths for progressively higher diffusivities can be found along dislocation-pipes, grain boundaries, and surfaces.
  - Grain boundaries between layers in nanocrystalline nanolaminate materials provides such features as needed for enhanced diffusion.
- The $\check{D}$(B) value decreases at both longer and shorter nanolaminate wavelengths.
  - A possible cause is that the enhanced diffusion from the grain boundary mechanism diminishes as the boundary length between interfaces becomes too long; or is inhibited by strain energy effects that are predominate at shorter wavelengths.

Discussion

Sandia National Laboratories

- Nonlinear diffusion effects will shift maximum growth to shorter wavenumbers, i.e. longer wavelengths, whereas strain energy will slow growth.
  - The interface-induced strain effect is more pronounced at longer wavenumbers, i.e. shorter wavelengths.
  - The maximum amplification for growth can shift to short wavenumbers with a further decrease of **T** below the spinodal.
  - *Thus, the further **T** is decreased below the chemical spinodal, we can expect the shape of the **R**(B) versus **B** curve to become progressively more bimodal as a consequence of the β-dependence of strain energy.*
- A lack of grain growth, i.e. recrystallization, implies the role of grain-boundary motion induced diffusion is not significant, whereas the use of grain boundaries and dislocation pipes provide paths for accelerated atomic transport between the layers of the nanolaminate.

Summary.1

Sandia National Laboratories

- The decomposition of a one-dimensional composition wave in Cu-Ni(Fe) nanolaminate structures is quantified using x-ray diffraction to determine the kinetics of interdiffusion.
  - A negative interdiffusivity is found for each sample aged at room temperature over a composition wavelength range of 2.1–10.6 nm.
- *Additional effects* are revealed as a result of the decomposition process over long time periods, such as a bifurcation of the wavelength for maximum growth.
  - *The competing effects of time, and the further suppression in temperature below the chemical spinodal for a strain layered structure produce an apparent bimodal distribution of the amplification factor* ***R*** *with wavenumber* β.

Summary.2

Sandia National Laboratories

- A diffusivity value **Ď** of 1.77×10^{-24} $cm^2 \cdot s^{-1}$ is determined for the Cu-Ni(Fe) alloy system – perhaps, the first such measurement at a ratio of melt-to-test temperature that's >5.
  - Although **Ď** is extremely small, it's several orders of magnitude greater than the value extrapolated from bulk diffusion.
- Operative diffusion mechanisms may include the possible effects of short-circuit diffusion through interlayer grain boundaries.
- For further reference about this topic…
  - Jankowski A F (2018) Interdiffusion at room temperature in Cu-Ni(Fe) nanolaminates. *Coatings 8:225-1-16*.
  - Jankowski A F (2015) Strain energy effects in the spinodal decomposition of Cu-Ni(Fe) nanolaminates coatings. *Coatings 5:246-262*.
  - Jankowski A F, Tsakalakos T (1989) Phase Stability by the Artificial Concentration Wave Method. *Metall. Trans. A 20:357-362*.